Journal of Applied Mechanics and Technical Physics, Vol. 48, No. 1, pp. 85–90, 2007

THERMAL AND DYNAMIC CHARACTERISTICS OF THE SEPARATED FLOW BEHIND A FLAT RIB WITH DIFFERENT ANGLES OF ALIGNMENT TOWARD THE FLOW

V. I. Terekhov, N. I. Yarygina, and Ya. I. Smulsky

UDC 536.24

Results of an experimental study of a turbulent flow past a flat rib with different angles of alignment toward the flow and with different rib heights are presented. The angle of rib alignment toward the flow is varied within $\varphi = 50$–$90°$. Vortex formation is visualized, and the coordinates of the reattachment line are determined. It is demonstrated that a decrease in the angle φ forms a reattachment region and makes the flow behind the rib more three-dimensional. Pressure coefficients are measured in different longitudinal sections of the channel behind the rib with a varied angle of rib alignment φ. Temperature fields on the surface behind the rib are measured by means of an infrared imager and by thermocouples, and the corresponding heat-transfer coefficients are calculated. The effect of the angle of rib alignment toward the flow and the rib height on dynamic and thermal characteristics of the separated flow is analyzed.

Key words: *turbulent flow, rib alignment, three-dimensional separated flow.*

Introduction. Heat transfer in channels of various devices used in power engineering is often intensified with the help of various obstacles, e.g., flat ribs. In a separated flow, both upstream and downstream of the rib, generation of large-scale vortex structures and interaction of coherent structures with the wall promote intensification of heat transfer on the wall. At the same time, the presence of obstacles leads to an undesirable increase in pressure losses. Thus, the task is to increase heat transfer and simultaneously reduce pressure losses. To solve this problem, one has to study the physical mechanisms of controlling vortex formation in separated flows and carefully measure the dynamic and thermal characteristics in a system of ribs and behind a single obstacle, in particular, behind a single rib.

Separated turbulent flow behind a flat obstacle aligned at an angle to the flow has some specific features, as compared to the flow behind an obstacle placed perpendicular to the flow. One of such features is a significant amplification of heat transfer [1–4]. This phenomenon is more and more widely used in engineering, for instance, for effective cooling of turbine blades or for increasing heat output in heat exchangers. As the obstacle is aligned at an angle to the free stream, the flow is three-dimensional. Numerical calculations of three-dimensional separated turbulent flows require large computational resources and do not ensure a necessary accuracy. In modeling oblique flows, a question arises whether there are regions and directions with invariant values of both dynamic and thermal characteristics, which is particularly important in the case of a single obstacle.

There are few papers that describe experimental investigations of the flow structure behind a single obstacle aligned at an angle to the flow, and there are even fewer papers where the thermal characteristics under these conditions are studied. Hancock and McCluskey [5] considered the flow behind a rib aligned at an angle $\varphi = 65°$ to the flow and compared the results with the data for $\varphi = 90°$. The components of the mean and fluctuating characteristics of the flow were determined. It was found that the distributions of velocity and streamwise fluc-

Kutateladze Institute of Thermophysics, Siberian Division, Russian Academy of Sciences, Novosibirsk 630090; terekhov@itp.nsc.ru. Translated from Prikladnaya Mekhanika i Tekhnicheskaya Fizika, Vol. 48, No. 1, pp. 103–109, January–February, 2007. Original article submitted December 27, 2005; revision submitted February 6, 2006.

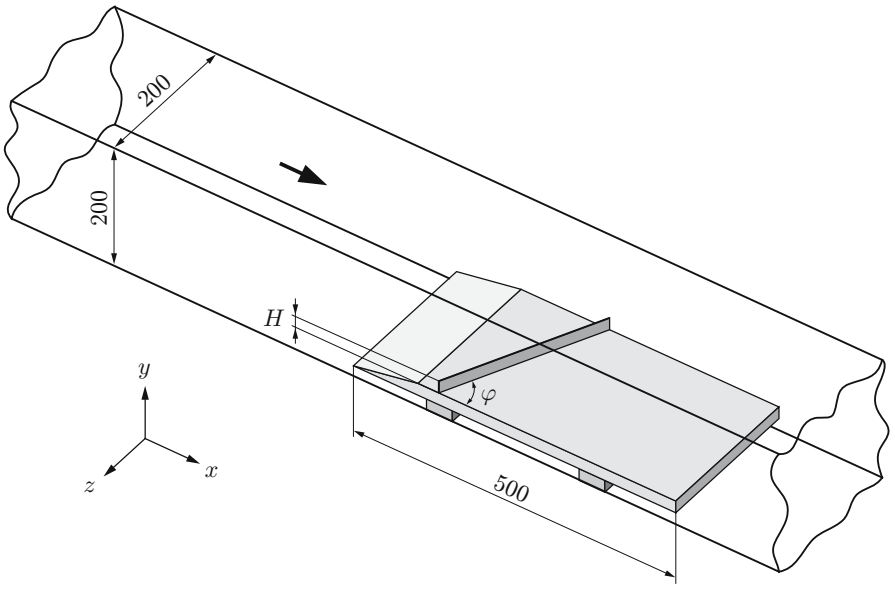

Fig. 1. Sketch of the test facility.

tuations of velocity in the direction perpendicular to the obstacle preserve their invariance until they reach the reattachment line. Invariance of shear stresses under the same conditions as in [5] was demonstrated in [6]. Okita et al. [7] considered the mean velocity fields and determined the pressure and friction coefficients in the flow around an obstacle aligned at an angle $\varphi = 20°$ to the flow. A self-similar pressure distribution along the rib was obtained. Mahmood et al. [8, 9] analyzed the flow in a rather narrow channel with a system of oblique ribs on the bottom and on the opposite wall. It was shown that heat transfer at high Reynolds numbers can be increased approximately by a factor of 2 in a channel with straight ribs on the wall and by a factor of 3 in a channel with oblique ribs. The efficiency becomes substantially higher as the difference in temperatures between the heated wall and the flow increases. Chyu and Wu [10] analyzed the combined effect of the angle of rib alignment, rib height, and distance between the ribs on mass transfer. It was shown that ribs aligned at an angle to the flow are more efficient from the viewpoint of heat-transfer intensification if the distance between the ribs is sufficiently large.

The goal of the present work was to continue the study of dynamics and heat transfer of a separated flow behind a flat obstacle with the angle of alignment of the obstacle toward the flow and the obstacle height varied in wide ranges.

Test Conditions. The experiments were performed in a wind tunnel based at the Institute of Thermophysics of the Siberian Division of the Russian Academy of Sciences. The facility has a rectangular channel 200×200 mm, which is 1000 mm long. A model 500 mm long was placed into the channel at a distance of 18 mm from the lower wall (Fig. 1). The stepped nose of the model approximately 100 mm long formed a turbulent boundary layer approximately 10 mm thick with the velocity distributed as 1/7 [11]. Two models of identical size were used to measure the thermal and dynamic characteristics of the model. Both models were made of a fabric-based laminate sheet 20 mm thick. The thermal model was heated by a strip heater made of aluminum foil in the regime of a constant heat flux on the wall $q_{\mathrm{w}} = \mathrm{const}$. There were thermocouples flush-mounted in the central section along the flow. The dynamic model had pressure taps spaced by 10 mm in five longitudinal sections over the channel span. The rib was attached to the model surface. The angle of rib alignment toward the flow φ was varied from 50 to 90° with a step of 10°, and the distance from the leading edge of the model to the center of the rib was 197 mm. Ribs of height $H = 6$, 10, and 20 mm were used for $\varphi = 60°$. In the remaining cases, the rib height was 20 mm. In most experiments, the free-stream velocity was 20 m/sec. The corresponding Reynolds number based on the rib height was $\mathrm{Re}_H = UH/\nu = 1.2 \cdot 10^4$, $2.6 \cdot 10^4$, and $3.9 \cdot 10^4$ (U is the free-stream velocity and ν is the kinematic viscosity).

For the separated flow on the surface behind the rib to be visualized by the oil-film technique, one more model was used; this model had the same size as the thermal and dynamic models and was covered by a Plexiglas layer 3 mm thick. The fluid used for visualization was a mixture of black offset paint and lamp oil.

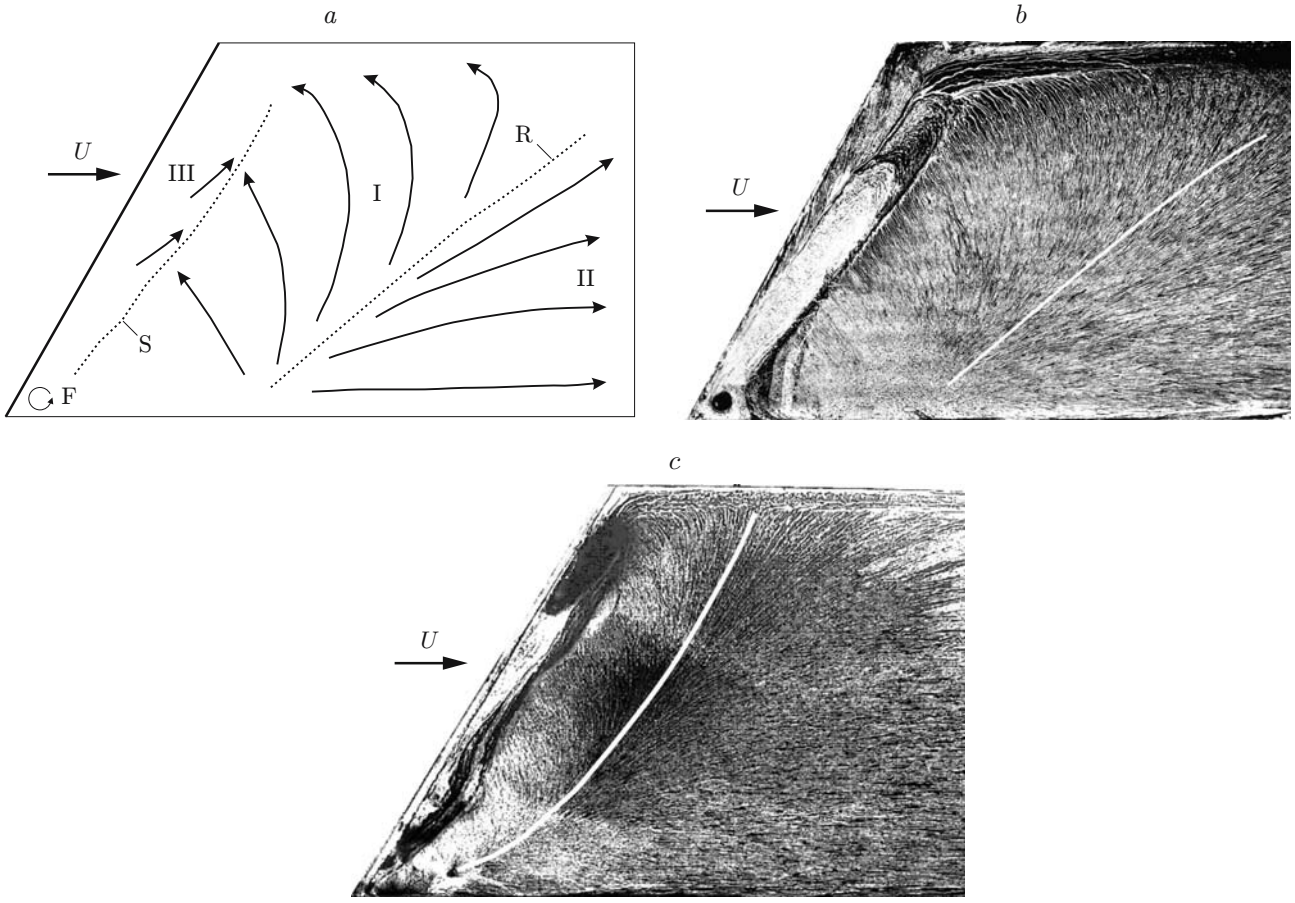

Fig. 2. Flow pattern behind a rib aligned at an angle $\varphi = 60°$: sketch of the flow for $H = 20$ mm (a) and results of oil-film visualization for $H = 20$ (b) and 6 mm (c); the regions indicated in the figure are the recirculation region (I), the relaxation region (II), and the region of the secondary flow and secondary vortex structures (III); the letters F, S, and R indicate a singular point of the "focus," a singular line of the "saddle" type, and the line of reattachment, respectively.

Test Results. Detailed visualizations of the flow behind a rib mounted across the flow were performed in [11–13]. It was found that the flow behind the perpendicular rib is symmetric, clearly expressed vortices are observed in the corners, and the reattachment line is almost parallel to the rib. As the angle of the flat rib decreases, the flow becomes asymmetric. A sketch of the flow behind an oblique rib with the basic regions is shown in Fig. 2a. For $\varphi < 90°$, the corner vortex near the acute corner φ is smaller than that in the case $\varphi = 90°$, and the vortex near the obtuse corner become smeared and increases in size, specially if a high obstacle is used (Fig. 2b).

Behind ribs of moderate height (for all angles), the line of reattachment has a segment parallel to the rib, which occupies almost half of the channel span in the case $H = 6$ mm and $\varphi = 60°$ (Fig. 2c). The flow characteristics in all sections parallel to the rib can be expected to be identical on this segment.

Behind high ribs, the line of reattachment, where the flow is separated into backflow and attached flow, becomes nonparallel to the rib, which is caused by a stronger influence of the side walls. Thus, for a flow behind a rib with $H = 20$ mm, the maximum difference in the flow structure from the case with $\varphi = 90°$ is reached at $\varphi = 50°$. The angle between the line of reattachment and the main flow is approximately equal to 45°. The line of reattachment behind an oblique rib is a smoother divergence line. It does not display Taylor–Görtler vortices, as in the case $\varphi = 90°$ [11]. The results of visualizations also showed that there is a clearly expressed crossflow along the line of reattachment. As the angle φ decreases, the distance between the rib and the line of reattachment x_{rib} decreases: for $\varphi = 50°$, almost by a factor of 2 in the central section of the channel and by a factor of 3 in the region adjacent to the acute corner. The values of x_{r}/H in the central section of the plate in the streamwise direction for different angles of rib alignment are listed in Table 1.

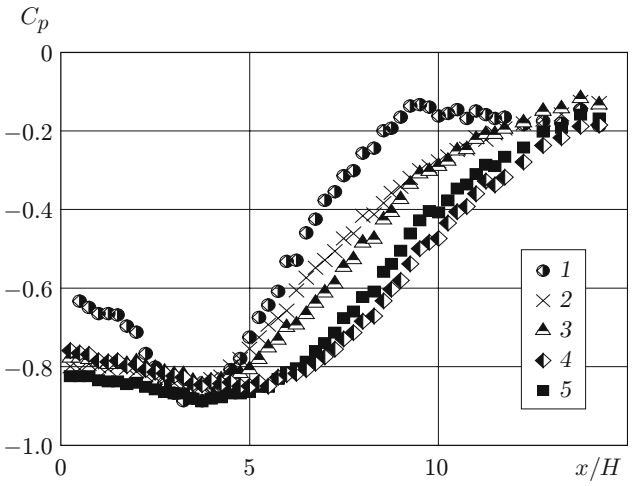

Fig. 3

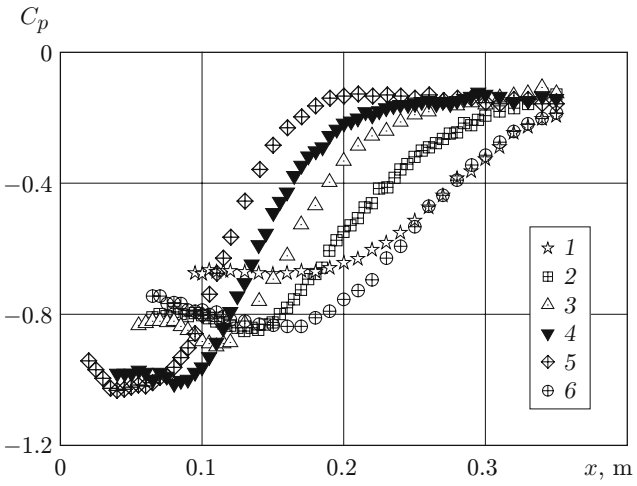

Fig. 4

Fig. 3. Distributions of the pressure coefficient in the central section for $\varphi = 50$ (1), 60 (2), 70 (3), 80 (4), and 90° (5).

Fig. 4. Distributions of the pressure coefficient in five longitudinal sections over the channel span: $z = -50$ (1), 0 (2), 25 (3), 50 (4), and 75 mm (5); points 1–5 refer to $\varphi = 60°$ and points 6 refer to $\varphi = 90°$.

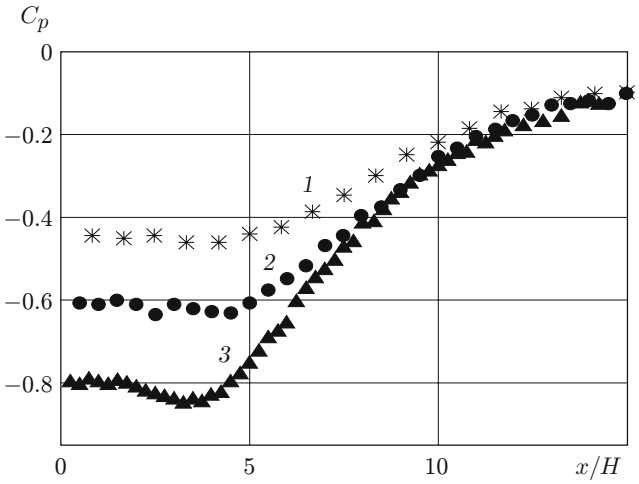

Fig. 5

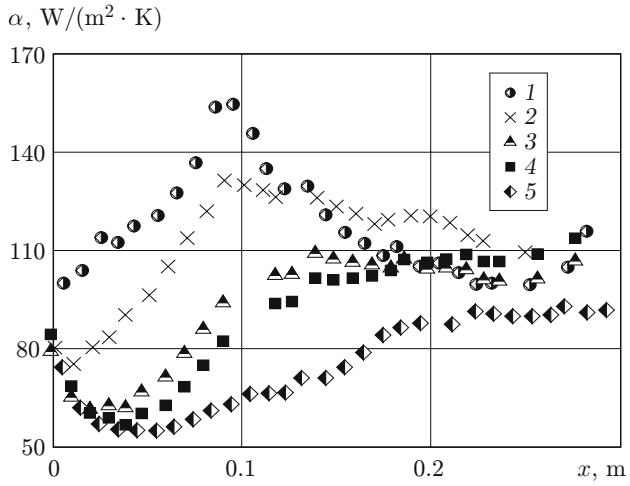

Fig. 6

Fig. 5. Pressure coefficient C_p versus the rib height for $\varphi = 60°$ and $H = 6$ (1), 10 (2), and 20 mm (3).

Fig. 6. Distributions of the heat-transfer coefficient along the channel for different values of the angle $\varphi = 50$ (1), 60 (2), 70 (3), 80 (4), and 90° (5).

A decrease in the separation-region size also leads to a decrease in the pressure-recovery region. The coordinates of the maximum pressure coefficients are given in Table 1. Figure 3 shows a typical distribution of the pressure coefficient $C_p = 2(p_i - p_0)/(\rho U^2)$ in the central longitudinal section of the model behind a rib 20 mm high with a varied angle φ (p_i is the pressure on the wall and p_0 and U are the reference pressure and velocity in the core flow above the rib). With decreasing φ, the pressure in the central section is recovered earlier than in other sections. The angle of attack of the flow, however, violates invariance of the pressure distribution over the

TABLE 1

Typical Dimensionless Distances
of the Recirculation Region along the Central Section over the Channel Span

φ, deg	$x_{\alpha,\max}/H$	x_{rib}/H	$x_{C_p,\max}/H$
50	4.0	7.5	9.3
60	4.5	9.5	11.3
70	7.0	10.25	12.3
90	11.0	16.5	17.0

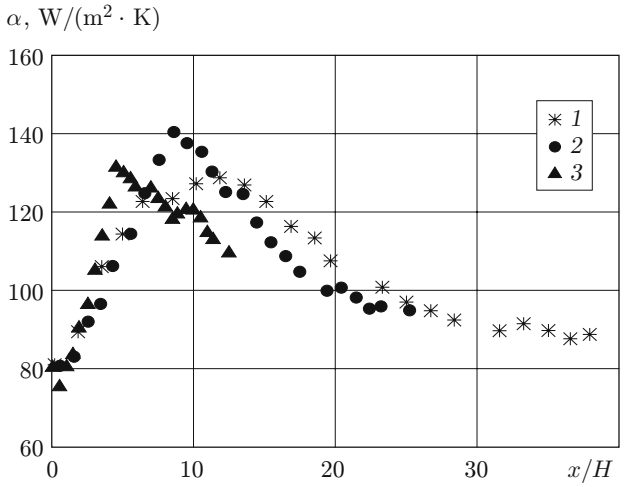

Fig. 7. Distributions of the heat-transfer coefficient along the channel for $\varphi = 60°$ and different heights of the rib: $H = 6$ (1), 10 (2), and 20 mm (3).

channel span (Fig. 4). The transverse coordinate z is counted from the channel center. For $\varphi = 90°$, the pressure distributions in all sections coincide. For low angles φ, the pressure is rapidly recovered in the region adjacent to the acute corner, whereas the pressure growth is rather slow in the region adjacent to the obtuse corner (as it occurs for $\varphi = 90°$). Thus, the length needed for pressure recovery is equal to or smaller than the length needed for pressure recovery at $\varphi = 90°$. The greatest difference in pressure is observed for low angles of rib alignment in the region adjacent to the acute corner. The effect of the rib height on the distribution of C_p in the central section over the channel span was examined for $\varphi = 60°$ (Fig. 5). As the rib height increases, the maximum rarefaction increases, and the dimensionless distance between the rib and the coordinate where the maximum pressure coefficient $C_{p,\max}$ is reached remains almost constant.

Behind the oblique rib, the thermal characteristics are close to the dynamic ones. In the present experiments, the temperature distributions along the channel centerline were obtained by thermocouples, and the temperature distributions in the entire region behind the rib were obtained by an infrared imager. Based on these distributions, the local heat-transfer coefficients were calculated.

The distribution of the heat-transfer coefficient α is similar to the distribution of the pressure coefficient C_p (Fig. 6). As the angle of rib alignment decreases, the maximum value of the heat-transfer coefficient increases, and the coordinate of this maximum $x_{\alpha,\max}$ approaches the rib. For $\varphi = 90°$, the point $x_{\alpha,\max}$ is substantially closer to the rib than the reattachment point x_{rib} and the coordinate of the pressure maximum $x_{C_p,\max}$. For low values of φ, the distance to the point of the maximum heat-transfer coefficient decreases more significantly than the distance to the point of the maximum pressure and the length of the reattachment region. For $\varphi = 50°$, the local maximum of the heat-transfer coefficient in the mid-section is approximately 70% higher than that for $\varphi = 90°$. The rib height exerts different effects on the pressure and heat-transfer coefficients; the influence of the rib height on the heat-transfer coefficient is rather weak (Fig. 7).

Conclusions. The effect of the angle of rib alignment toward the main flow ($\varphi = 50$, 60, 70, 80, and 90°) on vortex formation, pressure fields, and heat transfer for different Reynolds numbers (based on the rib height) $\mathrm{Re}_H = 1.2 \cdot 10^4$, $2.6 \cdot 10^4$, and $3.9 \cdot 10^4$ is considered.

It is shown that a decrease in the angle of rib alignment toward the flow reduces the distances to the line of reattachment and to the points of the maximum pressure and heat-transfer coefficients, and this reduction is most significant in the region adjacent to the acute corner. The greatest difference between the angle of inclination of the line of reattachment to the flow direction and the angle of rib alignment is observed for a high rib.

For low values of φ, the pressure distributions are substantially nonuniform over the channel span; in this case, rarefaction in the region of the secondary vortex adjacent to the acute corner increases.

As the angle φ decreases, the maximum values of the heat-transfer coefficient increases (by a factor of 1.7 in the mid-section for $\varphi = 50°$). As the rib height increases, the pressure behind the rib also increases, whereas the heat-transfer coefficient changes only weakly.

This work was supported by the Russian Foundation for Basic Research (Grant Nos. 06-08-00300 and 04-02-16070).

REFERENCES

1. C.-O. Olsson and B. Sunden, "Experimental study of flow and heat transfer in rib-roughened rectangular channels," *J. Exp. Thermal Fluid Sci.*, **16**, No. 4, 349–365 (1998).
2. X. Gao and B. Sunden, "Heat transfer and pressure drop measurements in rib-roughened rectangular channels," *J. Exp. Thermal Fluid Sci.*, **24**, No. 1, 25–34 (2001).
3. J. C. Han and J. S. Park, "Developing heat transfer in rectangular channels with rib turbulators," *Int. J. Heat Mass Transfer*, **31**, No. 1, 183–195 (1998).
4. R. Kiml, S. Mochizuki, and A. Murata, "Effects of rib arrangements on heat transfer and flow behavior in a rectangular rib-roughened passage: Application to cooling of gas turbine blade trailing edge," *J. Heat Transfer*, **123**, No. 4, 675–682 (2001).
5. P. E. Hancock and F. M. McCluskey, "Spanwise-invariant three-dimensional separated flow," *J. Exp. Thermal Fluid Sci.*, **14**, No. 1, 25–34 (1997).
6. P. E. Hancock, "Measurements of mean and fluctuating wall shear stress beneath spanwise-invariant separation bubbles," *Exp. Fluids*, **27**, No. 1, 53–59 (1999).
7. Yu. Okita, K. Ayukawa, K. Nakamura, et al., "The flow over an inclined fence in a turbulent boundary layer," *Trans. Jpn. Soc. Mech. Eng., Ser. B*, **67**, No. 655, 645–650 (2001).
8. G. I. Mahmood, P. M. Ligrani, and S. Y. Won, "Spatially-resolved heat transfer and flow structure in a rectangular channel with 45° angled rib turbulators," in: *Proc. of the* ASME TURBO EXPO 2002 (Amsterdam, Netherlands, June 3–6, 2002), ASME, Amsterdam (2002); CD Paper No. Gt-2002-30215.
9. G. I. Mahmood, P. M. Ligrani, and K. Chen, "Variable property and temperature ratio effects on Nusselt number in a rectangular channel with 45 deg angled rib turbulators," *J. Heat Transfer*, **125**, No. 5, 769–778 (2003).
10. M. K. Chyu and L. X. Wu, "Combined effects of rib angle-of-attack and pitch-to-height ratio on mass transfer from a surface with transverse ribs," *J. Exp. Heat Transfer*, **2**, No. 4, 291–308 (1989).
11. V. I. Terekhov, N. I. Yarygina, and R. F. Zhdanov, "Heat transfer in turbulent separated flows in presence of high free-stream turbulence," *Int. J. Heat Mass Transfer*, **46**, No. 23, 4535–4551 (2003).
12. V. I. Terekhov, N. I. Yarygina, and Ya. I. Smulsky, "Three-dimensional turbulent separated flow behind a flat obstacle with different angles of alignment toward the flow," in: *Proc. of the* XXVII*th Siberian Thermophysical Workshop* (Novosibirsk, October 4–5, 2004), Inst. Thermophysics, Sib. Div., Russian Acad. of Sci., Novosibirsk (2004); CD Paper No. 146; ISBN 5-89017-027-9.
13. V. I. Terekhov, N. I. Yarygina, and Ya. I. Smulsky, "Three-dimensional turbulent separated flow behind a flat obstacle with different orientations relative to the flow," in: *Proc. of the 6th World Conf. on Experimental Heat Transfer, Fluid Mechanics, and Thermodynamics* (Matsushima, Japan, April 17–21, 2005); Tohoku Univ., Miyagi (2005), CD Paper No. 3-a-5.